ELSEVIER

Catalytic hydrogenation of benzene to cyclohexene on Ru(0 0 0 1) from density functional theory investigations[☆]

Chen Fan[a], Yi-An Zhu[a,*], Xing-Gui Zhou[a], Zhi-Pan Liu[b,*]

[a] UNILAB, State Key Laboratory of Chemical Engineering, East China University of Science and Technology, 130 Meilong Road, Shanghai 200237, China
[b] Shanghai Key Laboratory of Molecular Catalysis and Innovative Materials, Department of Chemistry, Fudan University, 220 HanDan Road, Shanghai 200433, China

ARTICLE INFO

ABSTRACT

The catalytic hydrogenation of benzene on transition metal surfaces is of fundamental importance in petroleum industry. With the aim to improve its efficiency and particularly the selectivity to cyclohexene, in this contribution we perform periodic density functional theory calculations to determine the potential energy surface in the hydrogenation of benzene on Ru(0 0 0 1). By following the Horiuti–Polanyi mechanism with a step-wise addition of hydrogen adatoms, we investigate the adsorption of all the possible reaction intermediates and identify the most favored adsorption configuration for each intermediate. In particular, the most stable isomer for the same C_6H_n (n = 8, 9, 10) species are revealed as the most conjugated isomers, which are consistent with those in the gas phase. The elementary hydrogenation reactions of the most stable intermediates are then investigated under different H coverage conditions: the reaction barriers are calculated to be 0.68–0.97 eV at the low H coverage and 0.32–1.14 eV at the high H coverage. The high H coverage reduces significantly the overall barrier height of hydrogenation. With the determined pathway, we propose that the hydrogenation of benzene on Ru(0 0 0 1) follows the mechanism with the step-wise hydrogenation of neighboring C atoms in the ring, i.e., 1–2–3. . . hydrogenation. The selectivity to cyclohexene on Ru is also discussed, which highlights the importance of the π mode adsorption of benzene and also the adverse effect of secondary reaction process involving the readsorption and hydrogenation of cyclohexene.

1. Introduction

Owing to the known carcinogenic property of benzene, the concentration of benzene in fuels is strictly limited, the removal of which is often conducted by catalytic hydrogenation [1]. In addition, the selective hydrogenation product, cyclohexene, is an important industrial intermediate used in producing adipic acid, nylon-6, nylon-66, polyesters and other fine chemicals [2]. The hydrogenation of benzene is often used as a model system for the hydrogenation of aromatic compounds. For these reasons, benzene hydrogenation has attracted much attention in recent years. Although it was generally accepted that benzene hydrogenation follows a Horiuti–Polanyi mechanism [3] with a step-wise addition of hydrogen atoms, there are several possibilities for each hydrogenation step except for the first and last one. For example,

di-hydrobenzene, tri-hydrobenzene and tetra-hydrobenzene have three possible isomers. Several transition metals show efficient catalytic activity for benzene hydrogenation (e.g., Pt [4–8], Pd [9,10], Ni [11–13], Ru [14,15]). Among them, Ru is a very special one since it shows much higher selectivity to cyclohexene than any other reported transition metals [2,3,14–16]. In this work, we investigate the benzene hydrogenation path on Ru(0 0 0 1) with the aim to provide deeper understanding on the activity and selectivity.

Experimentally, various techniques have been used to analyze the adsorption of benzene on transition metals, including Pt, Pd, Rh, Ni, Ru, Mo, Cu and Ag, such as low-energy electron diffraction (LEED) [17,18], high-resolution electron energy loss spectroscopy (HREELS) [19,20], near-edge X-ray adsorption fine structure (NEXAFS) [21], angle-resolved ultraviolet photoelectron spectroscopy (ARUPS) [22], temperature program desorption (TPD) [23,24], photoelectron diffraction (PED) [25], scanning tunneling microscopy (STM) [26] and work function measurements. It is generally found that at low coverages benzene adsorbs with its ring parallel to the surface through the interaction between the π electrons and the d states of the transition metal surfaces [27]. However, the favored adsorption site of benzene on different metal surfaces varies, and on some surface the exact adsorption site is still controversial. On Pt(1 1 1), the observations by spectroscopic techniques

were conflict with the direct microscopic techniques. The NEX-AFS results indicated that benzene is centered on the top site of Pt(1 1 1), i.e., the gravity center of the molecule is located above one Pt surface atom [21]. The ARUPS analysis proposed a hollow site adsorption [22], while the LEED analysis indicated that only bridge sites are preferred [28,29]. The STM analysis found three different images corresponding to those three adsorption sites [30]. On Ni(1 1 1), scanned energy mode PED determined that in the disordered phase, benzene is centered over a bridge site with the C–C bonds oriented in the (2 1 1) direction at low coverages, while in the ordered overlayer the benzene ring is centered over the hcp site with the C–C bonds oriented in the (1 1 0) direction at the saturated coverages [25]. On Ru(0 0 0 1), LEED analysis demonstrated that the hcp site is preferred at the coverages ranging from 0.083 to 0.143 ML [17]. Compared to the large database on benzene adsorption, much less attention has been paid to the partial hydrogenated intermediates. *In-situ* experiments with sum frequency generation vibrational spectroscopy showed that π-allyl c-C_6H_9, 1,3-cyclohexadiene and 1,4-cyclohexadiene were the surface species on Pt(1 1 1) at different temperatures, while π-allyl c-C_6H_9, 1,4-cyclohexadiene and cyclohexyl were observed on Pt(1 0 0) during the dehydrogenation and hydrogenation of cyclohexene [31].

Apart from the large number of experimental investigation, theoretical calculations have also been performed on the adsorption of benzene and hydrogenated benzene molecules on various transition metal surfaces. First-principles density functional theory (DFT) calculations have been used to investigate the chemisorption of benzene on Pt(1 1 1) [32–35], Pd(1 1 1) [34,35], Rh(1 1 1) [35], Ni(1 1 1) [36], Ni(1 1 0) [36]. On Pt(1 1 1) and Ni(1 1 1), the results indicated that the bridge site is the energetically most favorable, while on Pd(1 1 1) and Rh(1 1 1), benzene molecules have similar adsorption energies on bridge and hollow sites. However, on Ni(1 1 0) and Ni(1 0 0), the hollow site is predominantly preferred. As for the partial hydrogenated intermediates, Saeys et al. calculated the adsorption of 1,4-cyclohexadiene on Pt(1 1 1) and found that the adsorption at the bridge and hollow sites are both likely with the adsorption energies of 146 and 142 kJ/mol, respectively. The red shift of the axial C–H stretching frequency and the corresponding C–H bond lengthening were also observed [37]. Xu et al. investigated the adsorption of cyclohexene on Pt(1 0 0). They found that the hollow site is preferred and the C–C double bond of cyclohexene binds with one surface Pt atom through π interaction [38]. Yuan et al. investigated the adsorption of cyclohexene on hexagonal close-packed Ru(0 0 0 1). They also found the π mode adsorption is preferred on Ru(0 0 0 1). However, on the close-packed surfaces of fcc transition metals (e.g., Pt, Ni, Pd), cyclohexene appears to prefer the di-σ mode adsorption [39]. Morin et al. investigated the adsorption of the intermediates for first four hydrogenation steps of benzene to cyclohexene on Pt(1 1 1) and Pd(1 1 1). They found that on Pd(1 1 1) the most conjugated intermediates which are most stable in the gas phase are clearly preferred, while on Pt(1 1 1), the radical species which are highly unstable in the gas phase are substantially stabilized upon adsorption [34].

To the best of our knowledge, little theoretical work has been devoted to investigating the adsorption of benzene and its partial hydrogenated intermediates on Ru(0 0 0 1). In this work, we present detailed survey through periodic density functional theory calculations for the possible intermediates during the hydrogenation of benzene to cyclohexane on Ru(0 0 0 1). The most stable intermediates are revealed and their hydrogenation reactions are studied. Based on the computed potential energy diagram at both low and high H coverages, we propose the reaction mechanism of the hydrogenation of benzene to cyclohexane on Ru(0 0 0 1). Our results shed light on the key factors to improve the selectivity towards cyclohexene.

2. Computational details

In this work, all total energy DFT calculations were firstly carried out with the SIESTA package using numerical orbital atomic basis sets and Troullier–Martins norm-conserving scalar relativistic pseudopotentials [40–42]. The double zeta-plus polarization (DZP) basis set was employed for basis set expansion. The orbital-confining cut-off radii were determined by an energy shift of 10 meV. The energy cut-off for the real space grid used to represent the density was set to 150 Ry. With the initial structures provided with SIESTA, all the reported energies were finally converged using VASP package [43,44], in which the wavefunctions at each k-point is expanded with a plane wave basis set up to a kinetic cut-off energy of 400 eV and the interactions between valence electrons and ion cores were treated by Vanderbilt ultrasoft pseudopotentials [45,46]. The exchange-correlation functional used was the generalized gradient approximation method, known as GGA-PBE [47]. The Ru(0 0 0 1) surface was modeled by four layers of Ru atoms, and a vacuum layer as large as 12 Å was used in the direction of the surface normal to avoid periodic interactions. A large $p(4 \times 4)$ supercell was used to avoid the lateral interactions between adsorbate images. Brillouin zone integrations have been performed using a $3 \times 3 \times 1$ Monkhorst-Pack grid [48]. The bottom two layers of the Ru atoms were fixed, and the top two layers of the Ru atoms as well as the adsorbates were allowed to relax. To correct the zero point energy (ZPE), vibrational frequency calculations were carried out by the numerical finite difference method.

To compare the stability of the partial hydrogenated intermediates, the relative adsorption energy of the C_6H_{6+n} species was calculated with respect to the gas phase benzene and H_2, as done with Eq. (1):

$$\Delta E_{ads} = E_{C_6H_{6+n}/sur} - E_{sur} - E_{C_6H_6} - \frac{n}{2}E_{H_2} \tag{1}$$

where $E_{C_6H_{6+n}/sur}$, $E_{C_6H_6}$, E_{H_2} and E_{sur} are the DFT total energies of the surface with an adsorbed C_6H_{6+n} species, a benzene molecule in the gas phase, a H_2 molecule in the gas phase and the bare surface, respectively. Therefore, the adsorption energies of different adsorbed species can always be compared with respect to the same reference level. Negative adsorption energy corresponds to an energy gain process. The adsorption energy for H atom with respect to 1/2 gas phase H_2 is calculated to be −0.61 eV on Ru(0 0 0 1) and the fcc site is found to be the most favorable for H adsorption on Ru(0 0 0 1).

Transition states (TSs) of the catalytic reactions are searched by the constrained Broyden minimization method [49]. All degrees of freedom except for the constrained reaction coordinate are relaxed. The TSs are identified when (i) the forces on the atoms vanish and (ii) the energy is a maximum along the reaction coordinate, but a minimum with respect to all of the other degrees of freedom.

3. Results and discussion

3.1. Adsorption of benzene

In the gas phase the C–C and the C–H distance of benzene are calculated to be 1.40 and 1.09 Å, respectively, which are in good agreement with the experimental values of 1.40 and 1.08 Å [36]. The adsorption of benzene on bare Ru(0 0 0 1) surface is then investigated by placing the gravity center of benzene in several high-symmetry positions, including hcp, fcc and bridge sites (see Fig. 1). Five most stable adsorption configurations, namely hcpA, hcpB, fccA, fccB and briA are identified, as shown in Fig. 1 (fccA and fccB configurations are not shown since they are similar to hcpA and hcpB configurations). The adsorption energies of the five configurations are calculated to be −1.55, −1.59, −1.56, −1.39
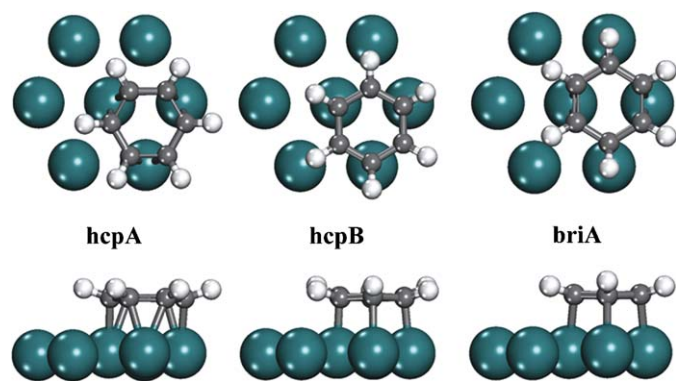
Fig. 1. Adsorption configurations (top view and side view) of benzene on high-symmetry sites of Ru(0 0 0 1). Large green balls denote Ru atoms, black balls denote C atoms and white balls denote H atoms.

Table 1
The energy change of d electrons (E_d as defined in Eq. (2)) of the surface atoms and the corresponding adsorption energies of benzene on Ru(0 0 0 1) and Pt(1 1 1).

Configuration	Ru(0 0 0 1)		Pt(1 1 1)	
	ΔE_{ads} (eV)	E_d (eV)	ΔE_{ads} (eV)	E_d (eV)
hcpA	−1.55	−1.80	−0.80	−8.98
hcpB	−1.59	−2.46	−0.44	−6.59
briA	−1.44	−1.38	−1.04	−9.57

and −1.44 eV (the detailed geometry parameters are shown in the Supplementary Information). It indicates that the hcpA, hcpB and fccB configurations are energetically more favorable for benzene adsorption on Ru(0 0 0 1). In all adsorption configurations, the carbon rings are parallel to the surface while the C–H bonds are tilted upward away from the surface. Our vibrational frequency analysis revealed that all the five adsorption configurations are the true energy minima with no negative vibrational mode.

The favored adsorption site of benzene on Ru(0 0 0 1) revealed here differs from what were found on other transition metal surfaces (e.g., Pt(1 1 1) and Ni(1 1 1)). On Pt(1 1 1) [32,33,35] and Ni(1 1 1) [25,36], benzene on bridge sites are reported to be 0.1–0.3 eV more stable than it on hollow sites, whereas on Ru(0 0 0 1) the hollow sites are 0.16 eV more favorable than the bridge sites. We notice that ethylene adsorption on Pt(1 1 1) [50] and Ru(0 0 0 1) [51] has the similar site-preference to benzene, which has been explained by the different adsorption mode. The di-σ mode adsorption (the C–C double bond is over two surface atoms) is preferred on Pt and thus the adsorption prefers the bridge site. By contrast, the π mode adsorption (the C–C double bond is over one surface atom) is favored on Ru and thus the hollow site adsorption is more stable. Generally speaking, the σ mode adsorption involves more surface atoms in bonding compared to the π mode adsorption. This can indeed be extended to understand that benzene at hcp sites are more stable than it at bridge sites on Ru(0 0 0 1).

To provide deeper insights from electronic structures, we have compared the density of states projected onto the d states (d-PDOS) of the surface atoms for benzene on Ru(0 0 0 1) and on Pt(1 1 1). By subtracting the d-PDOSs of the surface metal atom before and after the adsorption of benzene, we obtain the Δd-PDOS of Ru(0 0 0 1) and Pt(1 1 1), which are plotted in Fig. 2. For the cases of benzene adsorption on bridge sites, the Δd-PDOS is calculated by adding the Δd-PDOSs of the two σ bound surface atoms.

It can be seen that the Δd-PDOS around the Fermi level are strongly negative in all the six cases, which indicates that the surface atoms interact with the C atoms to form new covalent bonds and thus those d states shift to low-energy regions. Using Fig. 2, the energy change of d electrons (E_d) can be measured quantitatively from Eq. (2):

$$E_d = \int_{-\infty}^{E_F} \Delta n(\varepsilon)\,\varepsilon\,\mathrm{d}\varepsilon \qquad (2)$$

where $\Delta n(\varepsilon)$ (the y axis of Fig. 2) is the change of density of states of electrons in d levels at the energy ε. The E_d value can represent how the surface d states interact with the adsorbates. Based on the quantum mechanics picture of covalent bonding, it can be expected that the interaction of occupied d states with the antibonding empty states of adsorbates will lead to the stabilization of

the d states (e.g., σ mode bonding with benzene); whilst the empty d states to interact with the bonding states of adsorbates will lead to the destabilization of the d states (e.g., π mode bonding with benzene). The E_d values and the corresponding adsorption energies of benzene are shown in Table 1.

Our calculated adsorption energies of benzene on Pt(1 1 1) in hcpA, hcpB and briA configurations are found to be −0.80, −0.44 and −1.04 eV, respectively, which is very close to what is found by Morin et al. (−0.76, −0.41 and −1.04 eV) and Saeys et al. (−0.73, −0.53 and 1.06 eV) [32,33]. We can see that the adsorption energies of benzene on Ru(0 0 0 1) is generally larger than that on Pt(1 1 1), which is consistent with the general consensus that Ru is a more active metal than Pt because the d states of Ru being closer to the Fermi level can form a stronger bonding with benzene [52–54]. Importantly, in both cases Ru(0 0 0 1) and Pt(1 1 1), the calculated E_d follows the same order as the corresponding adsorption energies. The E_d values on Pt are systematically much larger than those on Ru. This implies that σ mode interaction dominates on Pt, where the d states are stabilized greatly at the expense of the weakening of benzene internal bonding. By contrast, there is a significant portion of π mode interaction on Ru due to the benzene π donation to empty Ru d states, which compensates the stabilizing effect of σ mode bonding. From the analysis, it can be concluded that π mode interaction on Ru plays a significant role for benzene bonding, whilst the σ mode interaction dominates on Pt(1 1 1).

Interestingly, it is noted that the hcpB configuration on Ru(0 0 0 1), in which only three shorter C–Ru bonds (~2.15 Å) are formed, is a little more stable (0.04 eV) than the hcpA configuration, in which six longer C–Ru bonds (~2.28 Å) are formed. This is indeed in consistent with experiment. Experimentally, Braun et al. performed LEED analysis on the adsorption of benzene on Ru(0 0 0 1). They found that at different coverages of benzene only the hcp adsorption site is favored, on which benzene molecule is centered above the hcp site with three of the six C atoms placed almost directly on the top of the three underlying Ru atoms involved in the hcp site and the remaining three C atoms placed above the neighboring fcc sites (corresponding to the hcpB configuration in our calculations) [17]. Furthermore, the C–C and C–Ru distances at their best fit geometry are 1.41/1.46 and 2.11 Å, also in good agreement with our calculated distances (1.44 and 2.17 Å), respectively. As the hcpA and fccA configurations are quite similar in geometry and adsorption energies, and the fccB configuration is much less stable than the hcpB configuration, only hcp sites are considered for the adsorption of the partial hydrogenated intermediates in the following.

3.2. Potential energy diagram

There are a large number of hydrogenated intermediates in hydrogenation of benzene to cylclohexane, including C_6H_7 (monohydrobenzene, BH), 1,2-C_6H_8 (1,3-cyclohexadiene, 13CHD), 1,3-C_6H_8 (1,3-di-hydrobenzene, 13DHB), 1,4-C_6H_8 (1,4-cyclohexadiene, 14CHD), 1,2,3-C_6H_9 (1,2,3-tri-hydrobenzene, 123THB), 1,2,4-C_6H_9 (1,2,4-tri-hydrobenzene, 124THB), 1,3,5-C_6H_9 (1,3,5-tri-hydrobenzene, 135THB), 1,2,3,4-C_6H_{10} (cyclohexene, CHE), 1,2,3,5-C_6H_{10} (1,2,3,5-tetra-hydrobenzene, 1235THB),
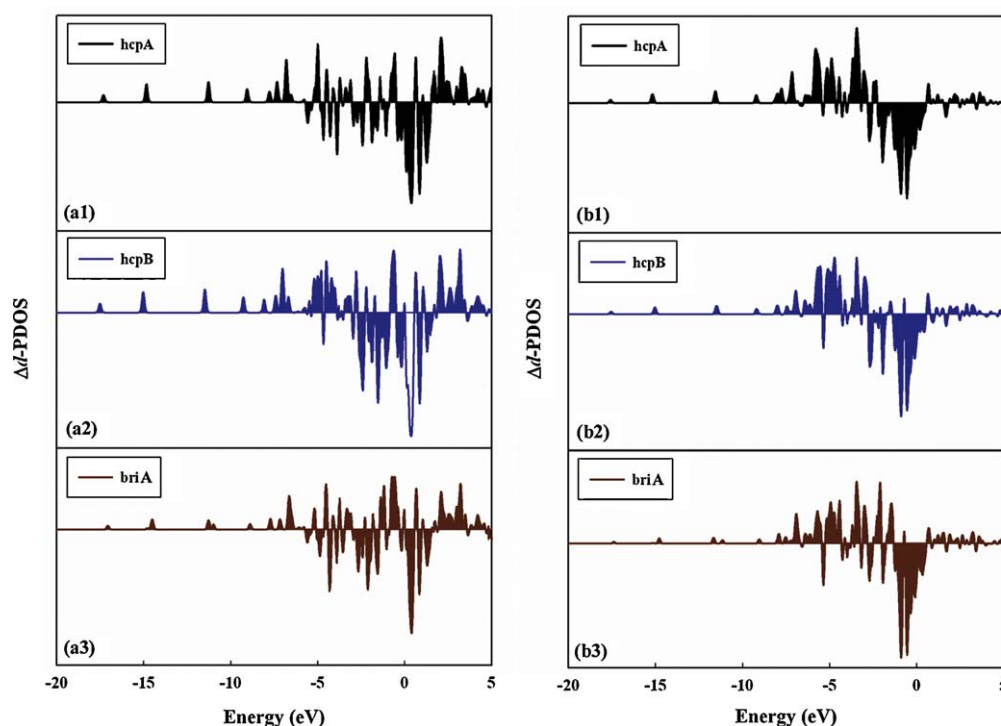
Fig. 2. Variation of d-projected density of states on the surface atoms before and after benzene adsorption. (a1)–(a3) hcpA, hcpB and briA on Ru(0 0 0 1). (b1)–(b3) hcpA, hcpB and briA on Pt(1 1 1). E_F corresponds to Fermi level which is set to be energy zero.

1,2,4,5-C_6H_{10} (1,2,4,5-tetra-hydrobenzene, 1245THB), C_6H_{11} (cyclohexyl, c-hexyl), C_6H_{12} (cyclohexane, CHA). For each intermediate, several possible adsorption configurations are considered in this work to identify the most energetically favorable adsorption configuration. The obtained main results are shown in Fig. 3 (the detailed geometry parameters and other unfavorable adsorption configurations are shown in the Supplementary Information). Some general trends for the adsorption of the intermediates are indentified. (i) For the closed shell molecules with C–C double bonds, π mode interaction is generally more favored than σ mode interaction. For example, the hcpA configuration of benzene, the 1,2-hcpA configuration of 13CHD and the 1,2,3,4-hcpA configuration of CHE are more favored than the bridgeB, 1,2-hcpB and 1,2,3,4-hcpB configurations, respectively (see Supplementary Information for details). (ii) For the radical fragments that are highly unstable in the gas phase are stabilized greatly upon adsorption, but this cannot fully compensate the intrinsic instability of the fragments. (iii) The H–Ru interactions also appear to contribute to the adsorption of the intermediates. In many cases, the H–Ru distances are rather short and the C–H bonds are stretched.

Using the calculated adsorption energies of the most stable configuration of each intermediate, we derive the potential energy diagram of the whole hydrogenation process, as shown in Fig. 4, where the ZPE of all the states has been included. The ZPE is essential for obtaining the potential energy diagram because there are six C–H bond formation from benzene to cyclohexane. The relative adsorption energetics and the ZPE data for the most stable species as utilized in Fig. 4 are listed in Table 2. The energy zero in the potential energy diagram is defined as the total energy of the gas phase benzene, hydrogen and the clean metal surface. In addition to the thermodynamics, we also searched for the reaction pathway of the benzene hydrogenation to CHA. As shown in Fig. 5, the most stable TSs have been located for the six hydrogenation steps. The calculated reaction barriers are listed in Table 3 and the ZPE of the TSs are listed in Table 2. From Fig. 4, we can

Table 2
The relative adsorption energies and ZPE (eV) of the most stable intermediates and the TSs at the low H coverage.

Species	$\Delta E_{ads}{}^a$ (eV)	ZPE (eV)	$\Delta E_{ads}{}^b$ (eV)
H_2 (g)[a]	0	0.26	0
Benzene (g)[b]	0	2.65	0
H	−0.61	0.15	−0.59
Benzene	−1.59	2.63	−1.61
BH	−1.57	2.95	−1.41
13CHD	−1.56	3.23	−1.25
123THB	−1.87	3.56	−1.36
CHE	−1.89	3.82	−1.26
c-hexyl	−2.07	4.14	−1.25
CHA	−2.80	4.54	−1.71
TS1	−1.38	2.81	−1.36
TS2	−1.45	3.14	−1.23
TS3	−1.52	3.41	−1.16
TS4	−1.80	3.75	−1.23
TS5	−1.77	4.10	−0.99
TS6	−1.84	4.42	−0.87

[a] ZPE corrections are not included.
[b] ZPE corrections are included.

see that the most conjugated intermediates which are most stable in the gas phase are still the most energetically favorable on the surface upon adsorption. For example, 13CHD, 123THB and CHE are the most stable isomers of di-hydrobenzene, tri-hydrobenzene and tetra-hydrobenzene, respectively. All the located TSs are quite similar in the sense that the reacting C and the H are over one Ru atom and the nascent C–H bonds are in the range of 1.4–1.6 Å. The calculated hydrogenation barriers of the elementary reactions are modest (0.68–0.97 eV) considering that the reaction is operated at 450 K. The highest reaction barrier step occurs at the final hydrogenation step from c-hexyl to CHA. Accordingly, we can deduce the reaction route from the thermodynamics and the kinetics results, which can be described as follows.

Firstly, benzene is converted to BH by adding the first H atom. Then, the attacking of the second H atom has three different path-

Table 3
The reaction barriers (E_a) and the reacting C–H distance of the six elemental steps of benzene hydrogenation to CHA on Ru(0001) at both the low and the high H coverages. ZPE corrections are included in E_a.

		TS1	TS2	TS3	TS4	TS5	TS6
Low H coverage	E_a (eV)	0.84	0.77	0.68	0.71	0.86	0.97
	d_{C-H} (Å)	1.60	1.47	1.45	1.48	1.37	1.44
High H coverage	E_a (eV)	1.14	0.62	0.37	0.42	0.32	0.63
	d_{C-H} (Å)	1.69	1.47	1.60	1.50	1.45	1.55

ways, since the di-hydrobenzene isomers have similar stabilities on the surface. Whatever the attacking position of the second H is, the dominant products of the third and forth hydrogenation steps are 123THB and CHE, respectively, due to their higher stabilities. Finally, CHE is hydrogenated to CHA through the intermediate of c-hexyl. Based on the calculated reaction barriers, it is expected that the hydrogenation of benzene to cyclohexane follows a mechanism with the step-wise hydrogenation of neighboring C atoms in the ring, i.e., 1–2–3... hydrogenation. It is noticed that two close-shell intermediates, 13CHD and CHE, are present during the hydrogena-

tion process. From our calculations, the adsorption energies of the 13CHD and CHE with respect to free 13CHD and CHE molecules are −1.60 and −0.64 eV, respectively. Considering that the typical reaction temperature of benzene hydrogenation on Ru(0001) is ∼450 K, one can expect that 13CHD is hard to desorb, while CHE can easily desorb as a product. The selectivity to CHE and to CHA depends on the energy barrier of the CHE hydrogenation to CHA step and also the adsorption energy of CHE under the reaction conditions, which will be addressed in the following at the high H coverage condition.
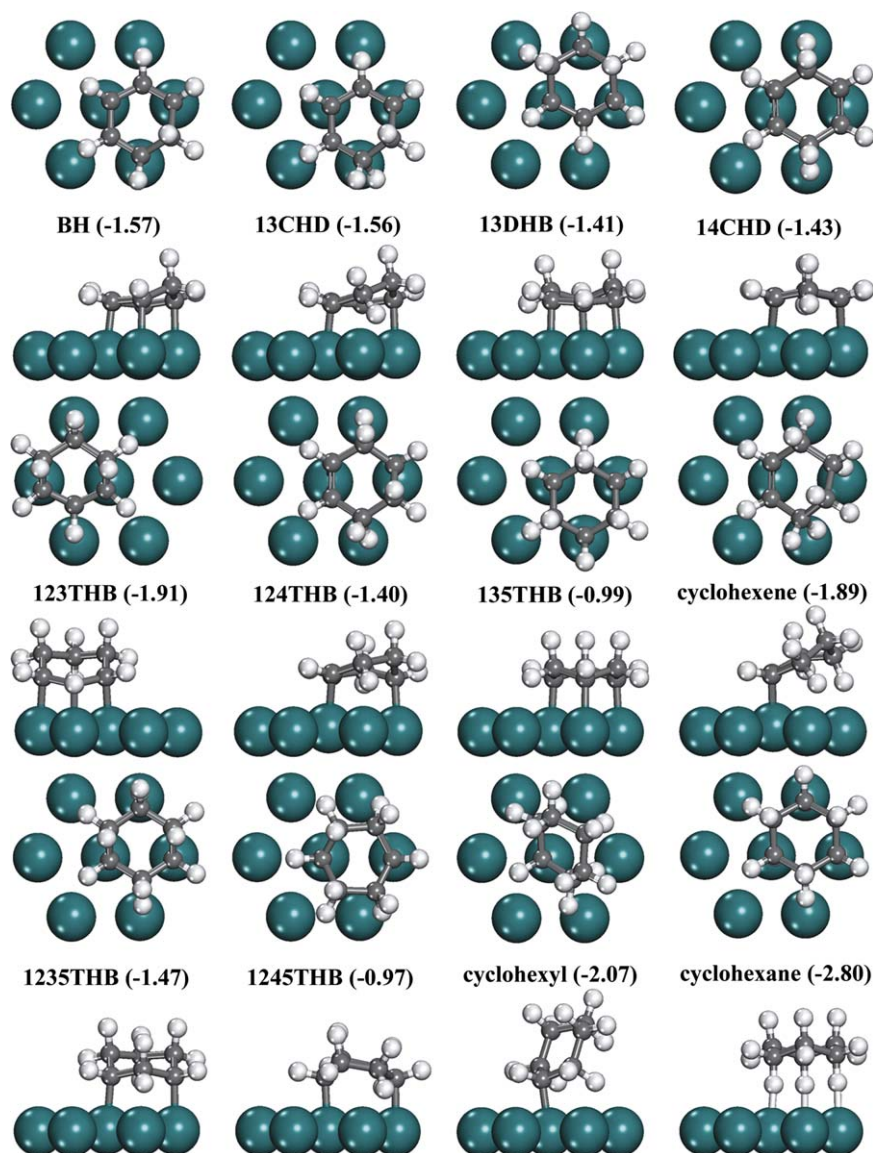

Fig. 3. The most stable adsorption configurations (top view and side view) and relative adsorption energies (eV) of all the hydrogenated intermediates. Large green balls denote Ru atoms, black balls denote C atoms and white balls denote H atoms. Adsorption energies (eV) are in the parentheses as calculated from Eq. (1) (ZPE corrections are not included).
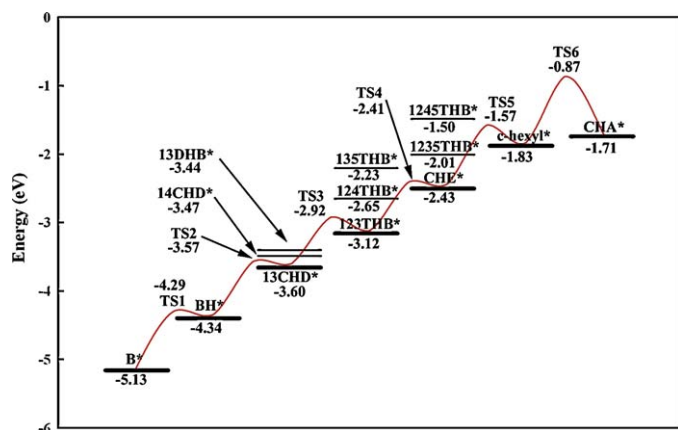
Fig. 4. The potential energy diagram of benzene hydrogenation to cyclohexane at low coverage (0.06 ML) of H on Ru(0 0 0 1). ZPE corrections have been included. The adsorption energy of a chemisorbed H is −0.59 eV. The chemisorbed H needed to balance the adsorption states have been omitted to simplify the notation. The red line is the lowest energy reaction route.
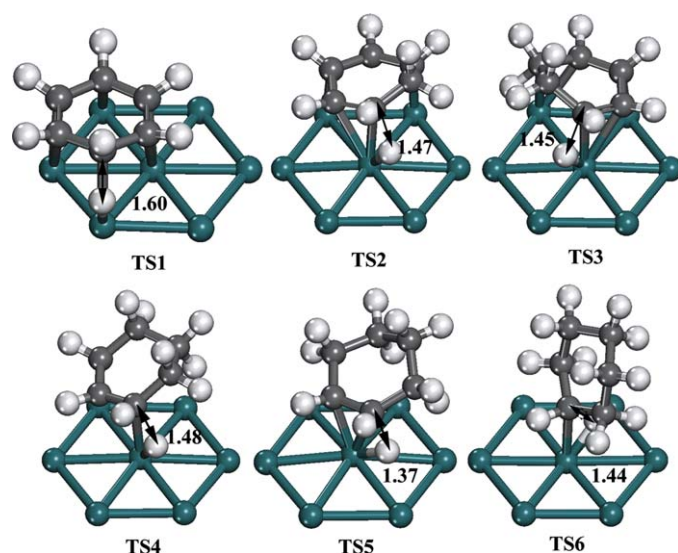

Fig. 5. The most stable TSs of the six elemental hydrogenation steps at low H coverages. Large green balls denote Ru atoms, black balls denote C atoms and white balls denote H atoms. The dissociative C–H distances (Å) are also labeled.

3.3. Surface coverage effect

It was shown in experiment that benzene hydrogenation to CHA on Ru metal catalyst is a fast reaction and can be finished in few minutes [3,14]. However, the energy diagram in Fig. 4 shows that the energy required from benzene to CHE (CHA) is more than 3 eV, which indicates that the reaction cannot occur under realistic conditions. This apparent inconsistency can be rationalized as follows. The energy diagram in Fig. 4 is obtained by assuming a low coverage condition, where a large $p(4 \times 4)$ Ru(0 0 0 1) supercell is utilized (the coverage of an adsorbate is low (0.06 ML)) and the lateral interaction between H and the intermediates is diminished in the infinite separation model. As a result, the adsorption energies of the benzene and H are rather large and the total energy change shown in Fig. 4 is much higher than the acceptable overall energy barrier. It should be mentioned that at the low coverage the CH activation and carbonaceous overlayer formation are likely to occur due to the decomposition of benzene. However, since the benzene hydrogenation occurs under the high pressure of hydrogen where the surface is covered with a high coverage of hydrogen, our low cov-

erage studies above are mainly for achieving better understanding at the high H coverage conditions, which will be addressed in the following.

Since the typical reaction temperature is ∼450 K and the partial pressure of H_2 is as high as ∼5 MPa, the surface coverage of the H under experimental conditions should be high and the H coverage effect could not be neglected. Therefore, it is essential to examine the adsorption of the intermediates at high H coverages. We first calculate the chemical potential (μ) of one H atom in the gas phase, which is defined as the half of the μ of the gas phase H_2. The chemical potential of H at 450 K and 5 MPa is −0.19 eV with respect to the total energy of 1/2 H_2, based on the standard thermodynamics data [55]. The detailed equations to derive the μ of the gas phase molecule at finite temperature and pressure can be found in previous publications [54,56,57]. Our calculated dissociative adsorption energy of H at coverage of 0.06 ML (−0.59 eV) is much larger than the μ of H at reaction conditions, which indicates that the adsorption of H is far from the chemical equilibrium. In fact, the calculated adsorption energy of H at the coverage of 1 ML (without other co-adsorbates) is −0.44 eV, still lower than the μ of H. Therefore, it can be expected that under the experimental conditions the Ru surface is in fact covered by a layer of H atoms. Hence, we investigate the adsorption of benzene and the most stable hydrogenated intermediates on the H-precovered surface. The coverage of H is set to be as high as possible (the subsurface H has not been considered in this work) and meanwhile enables the adsorption of benzene hydrogenation intermediates, which is about 0.81 (13/16) ML as the intermediate is found to occupy at least three sites of the surface. The adsorption configurations of benzene and CHE on the H-precovered Ru(0 0 0 1) surface is shown in Fig. 6. Other co-adsorption configurations and the corresponding adsorption energies are shown in the Supplementary Information. The TSs of the six elementary steps are then located at the high H coverage. The structures of the TSs are found to be similar to their counterparts at the low H coverage as shown in Fig. 5 with the distances of the reacting C–H compared in Table 3. The ZPE-included reaction barriers at the high H coverage are also listed in Table 3 (ZPE at the low H coverage is also utilized for that at the H coverage because ZPE of the intermediates is little affected by H coverage). The potential energy diagram of benzene hydrogenation to CHA at the high H coverage is shown in Fig. 7, which is very different from Fig. 4.

We find that at the high H coverage the adsorption energies of H, benzene and the hydrogenated intermediates are all reduced, which is apparently due to the large lateral interaction between H and the adsorbed intermediates. Interestingly, despite the large change in the potential energy surface, we note that the H coverage effect does not change the dominant reaction pathway. The stepwise hydrogenation of neighboring C atoms in the ring is still thermodynamically most favored.

Some general features of the hydrogenation process can be gleaned by comparing Fig. 4 and Fig. 7. (i) The increased H coverage has larger effects on the stability of the left-hand intermediates such as benzene than on that of the right-hand intermediates such as CHA. This can be rationalized as follows. First, the intermediates with more hydrogen added are gradually titled away from the surface, which leads to a smaller lateral interaction with the H. Second, the number of the chemisorbed H that is needed to balance the total energy of the states gradually decreases on going from the left to the right in Fig. 7. This also makes the right-hand states less affected by the H coverage. Most obviously, as CHA is only physically adsorbed on the surface, the energies of CHA state in Figs. 4 and 7 are rather constant (−1.71 in Fig. 4 and −1.63 eV in Fig. 7). (ii) The overall reaction energy change from benzene to CHE and CHA on Ru(0 0 0 1) drops sharply. At the high coverages, the reaction energy change from benzene to CHE is only 1.27 eV. The most unstable intermedi-
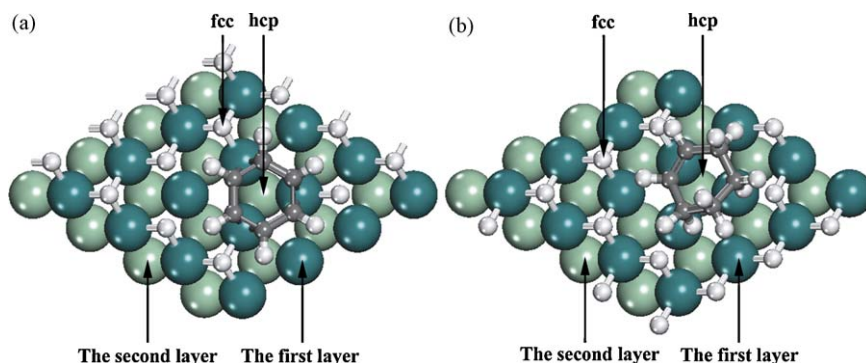
Fig. 6. Adsorption configuration of benzene (a) and CHE (b) on Ru(0 0 0 1) at the high H coverage (0.81 ML). Large green balls denote Ru atoms, black balls denote C atoms and white balls denote H atoms.
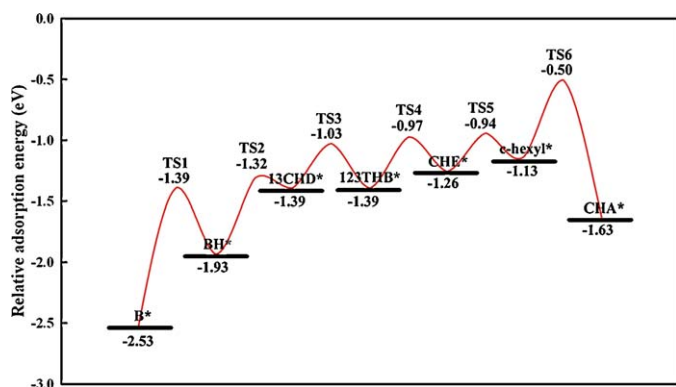

Fig. 7. The potential energy diagram of benzene hydrogenation to cyclohexane at the high H coverage (0.81 ML) on Ru(0 0 0 1). ZPE are included. The chemisorbed H needed to balance the adsorption states have been omitted to simplify the notation.

ate along the potential energy surface is c-hexyl* (see Fig. 7) and the energy change from benzene to c-hexyl* is 1.40 eV. In consistent, the overall barrier to produce CHA (-0.50 to (-2.53) = 2.03 eV) is higher than that to yield CHE (-0.97 to (-2.53) = 1.56 eV), which is beneficial to the selectivity towards CHE.

According to kinetics, the selectivity to CHE and to CHA depends on both the reaction barriers shown in Fig. 7 and the desorption/readsorption equilibrium of CHE. The readsorption of CHE will lead to the secondary reactions, where CHE competes with benzene for hydrogenation. For an ideal selective hydrogenation catalyst, the barrier of CHE to CHA should be higher than that of benzene to CHE, so that CHE can be produced without deep hydrogenation by tuning the reaction temperature. However, as shown in Fig. 7, even at the high H coverage condition, the barrier from benzene to CHE is 1.56 eV, which is still much larger than that of CHE to CHA (-0.50 to (-1.26) = 0.76 eV). This indicates that the readsorbed CHE, if available, can be easily hydrogenated at the reaction condition of benzene hydrogenation. Based on this and also considering that the complete hydrogenation to CHA is thermodynamically more favorable than to CHE even at high H coverages, the selectivity to CHE on pure Ru catalysts is expected to be not high. In fact, in order to achieve high selectivity of CHE, Ru catalysts are usually modified by certain additives (e.g., in ZnSO$_4$ solution or organic additives) or alloyed with other elements (e.g., Zn, Co, La, Fe, B) in experiment [3,16,58–61]. Without additives, pure Ru catalysts have poor selectivity to CHE with the main product being CHA.

Finally, it might be emphasized that our proposed reaction route of benzene hydrogenation on Ru(0 0 0 1) is different from that on Pt(1 1 1) proposed by Morin et al. and Saeys et al. [34,62]. They found that on Pt(1 1 1) hydrogenation occurs preferentially in the meta position of the methylene group and the dominant reaction pathway goes through the multiple radical species. In this path, 13CHD and CHE are not formed and the only product that can desorb is CHA. Apparently, this agrees with the fact that Pt-based catalysts show poor selectivity to CHE, and they are usually used for the complete hydrogenation [6–8]. On the other hand, a good catalyst for selective hydrogenation of benzene to CHE should therefore possess the property that the closed shell molecules should be more stable than the radical species upon adsorption. This is indeed the case on Ru as the π mode bonding plays important role together with the σ mode bonding. By this means, CHE, the selective hydrogenation product, could be involved in the dominant reaction pathway.

4. Conclusion

First-principles calculations are performed to determine the potential energy surface in the hydrogenation of benzene on Ru(0 0 0 1). We investigate the adsorption of all the possible intermediates on the surface, and obtain the potential energy diagram at both low and high H coverages. Our main conclusions are as follows. The most conjugated intermediates, e.g., 13CHD, 123THB and CHE, which are the most stable intermediates in the gas phase, are still favorable upon adsorption. From thermodynamics and kinetics calculations, we show that the hydrogenation of benzene to CHE on Ru(0 0 0 1) follows a mechanism with the stepwise hydrogenation of neighboring C atoms in the ring with the elementary hydrogenation barriers being 0.68–0.97 eV at the low H coverages and 0.32–1.14 eV at the high coverages. The effect of surface H coverage on the adsorption is found to be crucial. At low H coverage, the Ru surface shows no activity, since the overall barrier is too high for the hydrogenation reaction to occur under experimental conditions. As the H coverages increases, the adsorption energies of all the intermediates are highly reduced due to the large lateral interaction between the H and the intermediates. The selectivity to CHE has also been analyzed based on the potential energy profile. It shows that (i) a preferable π mode bonding between alkene and metal surface is the prerequisite for the selectivity towards CHE and (ii) at the high H coverage on Ru the overall barrier of CHE to CHA is still much lower than that of benzene to CHE, indicating that the secondary reaction involving the readsorption and hydrogenation of CHE will lower the selectivity to CHE markedly.

cational Development Foundation through Chenguang plan (No. 2007CG41).

Appendix A. Supplementary data

References

[1] B.H. Cooper, B.B.L. Donnis, Appl. Catal. A 137 (1996) 203.
[2] H. Nagahara, M. Ono, M. Konishi, Y. Fukuoka, Appl. Surf. Sci. 121–122 (1997) 448.
[3] J. Struijk, M. d'Angremond, W.J.M.L.-d. Regt, J.J.F. Scholten, Appl. Catal. A 83 (1992) 263.
[4] K.M. Bratlie, M.O. Montano, L.D. Flores, M. Paajanen, G.A. Somorjai, J. Am. Chem. Soc. 128 (2006) 12810.
[5] K.M. Bratlie, Y.M. Li, R. Larsson, G.A. Somorjai, Catal. Lett. 121 (2008) 173.
[6] S.L. Lu, W.W. Lonergan, J.P. Bosco, S.R. Wang, Y.X. Zhu, Y.C. Xie, J.G. Chen, J. Catal. 259 (2008) 260.
[7] N.H.H. Abu Bakar, M.M. Bettahar, M. Abu Bakar, S. Monteverdi, J. Ismail, M. Alnot, J. Catal. 265 (2009) 63.
[8] S.L. Lu, W.W. Lonergan, Y.X. Zhu, Y.C. Xie, J.G.G. Chen, Appl. Catal. B 91 (2009) 610.
[9] A. Horvath, A. Beck, Z. Koppany, A. Sarkany, L. Guczi, J. Mol. Catal. A: Chem. 182 (2002) 295.
[10] P.H. Jen, Y.H. Hsu, S.D. Lin, Catal. Today 123 (2007) 133.
[11] K.C. Metaxas, N.G. Papayannakos, Chem. Eng. J. 140 (2008) 352.
[12] M.H. Peyrovi, M.R. Toosi, React. Kinet. Catal. Lett. 94 (2008) 115.
[13] P.G. Savva, K. Goundani, J. Vakros, K. Bourikas, C. Fountzoula, D. Vattis, A. Lycourghiotis, C. Kordulis, Appl. Catal. B 79 (2008) 199.
[14] J. Bu, J.L. Liu, X.Y. Chen, J.H. Zhuang, S.R. Yan, M.H. Qiao, H.Y. He, K.N. Fan, Catal. Commun. 9 (2008) 2612.
[15] J.L. Liu, L.J. Zhu, Y. Pei, J.H. Zhuang, H. Li, H.X. Li, M.H. Qiao, K.N. Fan, Appl. Catal. A 353 (2009) 282.
[16] J. Struijk, R. Moene, T.v.d. Kamp, J.J.F. Scholten, Appl. Catal. A 89 (1992) 77.
[17] W. Braun, G. Held, H.P. Steinruck, C. Stellwag, D. Menzel, Surf. Sci. 475 (2001) 18.
[18] A. Wander, G. Held, R.Q. Hwang, G.S. Blackman, M.L. Xu, P.d. Andres, M.A.V. Hove, G.A. Somorjai, Surf. Sci. 249 (1991) 21.
[19] S. Lehwald, H. Ibach, J.E. Demuth, Surf. Sci. 78 (1978) 577.
[20] F. Cemic, O. Dippel, E. Hasselbrink, Surf. Sci. 342 (1995) 101.
[21] M. Yimagawa, T. Fujikawa, Surf. Sci. 357–358 (1996) 131.
[22] J. Somers, M.E. Bridge, D.R. Lloyd, T. McCabe, Surf. Sci. 181 (1987) L167.
[23] J.M. Campbell, S. Seimanides, C.T. Campbell, J. Phys. Chem. 93 (1989) 815.
[24] C. Xu, Y.-L. Tsai, B.E. Koel, J. Phys. Chem. 98 (1994) 585.
[25] V. Schaff, P. Fernandez, K.-M. Hofmann, A. Schindler, Theobald, Surf. Sci. 348 (1996) 89.
[26] S.-L. Yau, Y.-G. Kim, K. Itaya, J. Am. Chem. Soc. 1996 (1996) 7795.
[27] F.P. Netzer, Langmuir 7 (1991) 2544.
[28] D.F. Ogletree, M.A.v. Hove, G.A. Somorjai, Surf. Sci. 183 (1987) 1.
[29] C.M. Mate, G.A. Somorjai, Surf. Sci. 160 (1985) 542.
[30] P.S. Weiss, D.M. Eigler, Phys. Rev. Lett. 71 (1993) 3139.
[31] K.M. Bratlie, L.D. Flores, G.A. Somorjai, J. Phys. Chem. B 110 (2006) 10051.
[32] C. Morin, D. Simon, P. Sautet, J. Phys. Chem. B 107 (2003) 2995.
[33] M. Saeys, M.F. Reyniers, G.B. Marin, M. Neurock, J. Phys. Chem. B 106 (2002) 7489.
[34] C. Morin, D. Simon, P. Sautet, Surf. Sci. 600 (2006) 1339.
[35] C. Morin, D. Simon, P. Sautet, J. Phys. Chem. B 108 (2004) 5653.
[36] F. Mittendorfer, J. Hafner, Surf. Sci. 472 (2001) 133.
[37] M. Saeys, M.F. Reyniers, G.B. Marin, M. Neurock, Surf. Sci. 513 (2002) 315.
[38] W.G. Xu, Z.F. Shang, G.C. Wang, J. Mol. Struct. 869 (2008) 47.
[39] P.Q. Yuan, B.Q. Wang, Y.M. Ma, H.M. He, Z.M. Cheng, W.K. Yuan, J. Mol. Catal. A: Chem. 301 (2009) 140.
[40] J.M. Soler, E. Artacho, J.D. Gale, A. Garcia, J. Junquera, P. Ordejon, D. Sanchez-Portal, J. Phys.: Condens. Mater. 14 (2002) 2745.
[41] J. Junquera, O. Paz, D. Sanchez-Portal, E. Artacho, Phys. Rev. B 64 (2001).
[42] N. Troullier, J.L. Martins, Phys. Rev. B 43 (1991) 1993.
[43] G. Kresse, J. Hafner, Phys. Rev. B 47 (1993) 558.
[44] G. Kresse, J. Hafner, Phys. Rev. B 49 (1994) 14251.
[45] G. Kresse, J. Hafner, J. Phys.: Condens. Mater. 6 (1994) 8245.
[46] D. Vanderbilt, Phys. Rev. B 41 (1990) 7892.
[47] J.P. Perdew, K. Burke, M. Ernzerhof, Phys. Rev. Lett. 77 (1996) 3865.
[48] H.J. Monkhorst, J.D. Pack, Phys. Rev. B 13 (1976) 5188.
[49] H.F. Wang, Z.P. Liu, J. Am. Chem. Soc. 130 (2008) 10996.
[50] G.W. Watson, R.P.K. Wells, D.J. Willock, G.J. Hutchings, J. Phys. Chem. B 104 (2000) 6439.
[51] J.M. Hill, R. Alcala, R.M. Watwe, J. Shen, J.A. Dumesic, Catal. Lett. 68 (2000) 129.
[52] B. Hammer, J.K. Nørskov, Surf. Sci. 343 (1995) 211.
[53] A. Ruban, B. Hammer, P. Stoltze, H.L. Skriver, J.K. Nørskov, J. Mol. Catal. A: Chem. 115 (1997) 421.
[54] Z.P. Liu, S.J. Jenkins, D.A. King, J. Am. Chem. Soc. 126 (2004) 10746.
[55] D.R. Lide, CRC Handbook of Physics and Chemistry, 79th ed., CRC Press, 1998.
[56] M.V. Bollinger, K.W. Jacobsen, J.K. Nørskov, Phys. Rev. B 67 (2003) 085410.
[57] D. Loffreda, Surf. Sci. 600 (2006) 2103.
[58] G.Y. Fan, R.X. Li, X.J. Li, H. Chen, Catal. Commun. 9 (2008) 1394.
[59] G.Y. Fan, W.D. Jiang, J.B. Wang, R.X. Li, H. Chen, X.J. Li, Catal. Commun. 10 (2008) 98.
[60] J.Q. Wang, Y.Z. Wang, S.H. Zhe, M.H. Qiao, H.X. Li, K.N. Fan, Appl. Catal. A 272 (2004) 29.
[61] S.C. Liu, Z.Y. Liu, Z. Wang, S.H. Zhao, Y.M. Wu, Appl. Catal. A 313 (2006) 49.
[62] M. Saeys, M.F. Reyniers, M. Neurock, G.B. Marin, J. Phys. Chem. B 109 (2005) 2064.